BATHYMETRY INVERSION IN THE SURF ZONE VIA ASSIMILATION OF REMOTELY SENSED WAVE BREAKING ENERGY DISSIPATION

Francisco Soto, Universidad Técnica Federico Santa María, francisco.sotos@usm.cl
Patricio Catalán, Universidad Técnica Federico Santa María, patricio.catalan@usm.cl

INTRODUCTION

The nearshore is the geographical band where oceans and lands interact. In spite of its limited extent, it is one of the areas humans show most concern to, as several activities take place there, ranging from recreational to political and economic, and also provides protection against environmental hazards that may affect hinterland. Hence, a good understanding and prediction capabilities of the nearshore are interesting not only from a scientific point of view but also to the general interest of society, with the eventual long-term goal of improving management and increasing safety.

Fundamental for these purposes is an accurate representation of bathymetry. Good estimates, in addition to reliable numerical models, might improve present prediction capabilities. This approach, that treats bathymetry as an input, is a forward problem. However, bathymetric estimates at hand usually lack the spatial and temporal resolution required, as they are not always measurable at the required operational rates and safe conditions. Sometimes they are completely absent.

Fortunately, as the influence of bathymetry on many coastal processes that have strong signatures on remote sensors, such as wave propagation and coastal currents, is fairly well understood, it is possible to pose an inverse problem, i.e., bathymetric inversion. In the last decades, mainly due to the outspread of digital cameras and other remote sensors, two main depth dependences have been exploited: wave celerity and wave breaking dissipation (Holman and Haller, 2013).

The former (e.g. Holman et al., 2013) uses signal processing techniques to estimate the phase propagation velocity and invert the linear dispersion relation to estimate depth. While showing good performance outside the surf zone, their accuracy degrades shoreward due to wave nonlinearities (Catalán and Haller, 2008) and the spurious acceleration measured by remote sensors when the imaging mechanism changes as waves break (Brodie et al., 2018). Others (e.g. Aarninkhof et al., 2005; van Dongeren et al., 2008) have used long exposure optical images of breaking waves to estimate patterns that are treated as dissipation proxies. Inverted depths are obtained in light of the difference between measurements and model predictions. This approach has had less attention, possibly due to the lack of a physical background to estimate dissipation, as this signal is contaminated by that arising from other phenomena such as remnant foam. Lately, hybrid methods have been developed too. These are capable of combining the previous and other variables that may depend on depth in intricate ways, using data assimilation tools. For instance, Wilson et al. (2014) used remote measurements of celerity and alongshore currents with very good results. The potential downside is the need to couple in situ data to drive the assimilation, affecting the benefit of a purely remote sensing estimate.

In this work, a data assimilation approach treating bathymetry as an uncertain model parameter, is introduced where direct dissipation estimates from remote sensing data are the unique data source. Two dimensional wave breaking dissipation fields are retrieved on a wave-by-wave basis with the algorithms of Díaz et al. (2018), who were able to reliably estimate breaking dissipation by removing spurious signals affecting electro-optical and microwave data.

In the following, insight about data acquisition and its processing until the estimation of two-dimensional dissipation fields is given. Next, the bathymetry inversion system is presented, followed by the results and their discussion. Conclusions are given in the last section.

DATA ACQUISITION AND PROCESSING

Data were collected at the U.S. Army Corps of Engineers Field Research Facility (FRF) near the town of Duck, NC, during the Surf Zone Optics experiment, from the 9th to the 15th of September 2010. These consist of optical and X band signals measured with Argus cameras (Holman and Stanley, 2007) and a marine radar (Catalán et al., 2011), respectively. Here, six synchronous and colocated 17min length records taken at the start of each hour, between 11 and 16hrs (EST) during 10th Sep. 2010, are considered.

To isolate the remnant foam signal and capture the roller geometry, these signals are merged following Díaz et al. (2018). For each pair of recordings, the joint histogram is calculated (Figure 1a), where high optical intensities are indicative of remnant foam and active breaking, and high radar backscatter of steepening and broken waves (Catalán et al., 2011). Then, the wave stage present in each pixel is classified using thresholds that are found looking for local minimum or maximum curvature in the marginal histograms (Panels b and c). The algorithm also allows book-keeping of the Lagrangian trajectories of the broken waves (not shown).

This information is used to calculate roller lengths in the wave propagation direction and is coupled to a model (Duncan, 1981; Dally and Brown 1995) to estimate the roller dissipation rate on a wave-by-wave basis. Finally, time-averaged dissipation fields are obtained for the 17min of observation (Figure 1f).

BATHYMETRY INVERSION SYSTEM

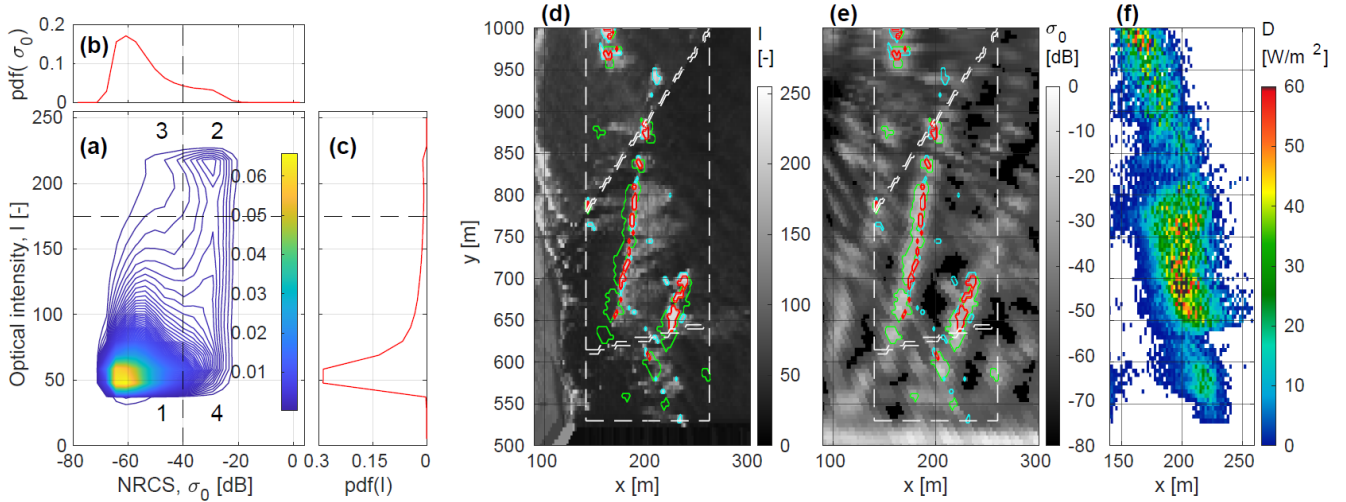The inversion system is based on a sequential ensemble-based data assimilation scheme that treats

Figure 1. Roller dissipation from remote sensing data. Joint histogram (a), marginal histogram of radar backscatter (b) and optical intensity (c). Dashed lines indicate thresholds that divide the JPDF in: 1. nonbreaking waves, 2. breaking waves, 3. remnant foam, 4. steepening waves. In panels (d) and (e) green, red and cyan lines confine pixels corresponding to steepening waves, breaking waves and remnant foam, respectively, over optical and X band snaps (shoreline at $x \approx 100m$). White dashed lines are cameras boundaries. Mean roller dissipation field at 15.00(EST) is shown in (f).

bathymetry as the only uncertain parameter of the model, which is conditioned to dissipation measurements every time they are available. This methodology largely follows the work of Wilson et al. (2014). The fundamental steps of the procedure are outlined below and in Figure 2:

1. An initial ensemble of $N = 200$ bathymetric realizations is defined.
2. A forward model is applied to each ensemble member with fixed wave boundary conditions for observational time t_i. Model outputs, i.e., roller dissipation, are used to form the background state ensemble.
3. Corresponding remote measurements at t_i are processed to estimate the roller dissipation along with its uncertainty, in the form of an ensemble of observations.

4. The background system state is conditioned to observations with an Ensemble Kalman filter, and an analyzed ensemble is produced.
5. To account for known shortcomings of the filter and eventually failed members, the ensemble is resampled and its spread is adjusted.
6. Before moving to the next observational time, by taking the corresponding rows of the ensemble, inversed depths and its uncertainty are estimated as the ensemble mean and its variance respectively. Then, the cycle is repeated from step 2.

As a result, several cycles of assimilation should retrieve improved estimates of bathymetry given the information provided by the observations and the model physics.

The initial bathymetric ensemble was modeled as an equilibrium beach profile to which perturbations sampled from a Gaussian distribution with length scales $L_x = L_y = 100/\sqrt{3}m$ and $\sigma_z = 0.5m$ (Wilson et al., 2014) were added.

Finally, the model used to simulate incident waves is SWAN (Booij et al., 1999), with default parameters, and forced with spectral measurements from the 8m-Array (Long, 1996). The only sink term considered is depth-induced wave breaking following Battjes and Janssen (1978), and tidal elevations are included as spatially constant offsets in the still water level for each model time. Further, wave spectral predictions are passed to a roller evolution model (Reiners et al., 2004) to compute the roller dissipation.

Figure 2. Bathymetry inversion system flow diagram.

RESULTS
In the course of the observational time window considered, significant wave height was around $0.85m$ and peak wave period approximately $T = 5s$. Wave spectra consisted of
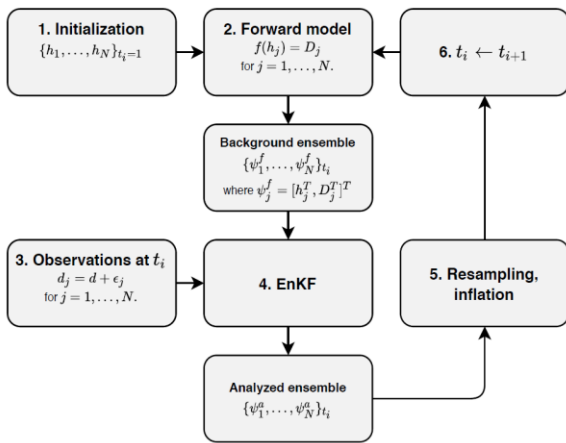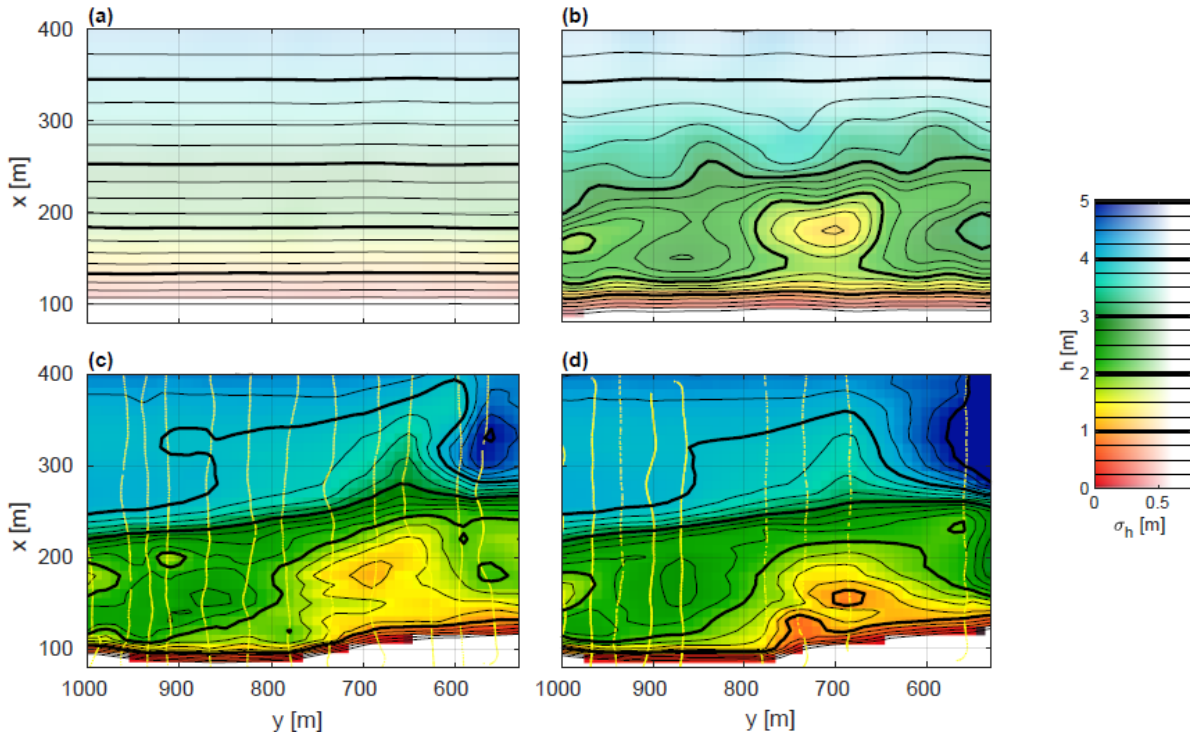
Figure 3. Results. Initial bathymetry (a), inverted bathymetry after 6 assimilation cycles during 10 Sep. (b), in situ measurements from 6 Sep. (c) and 15 Sep. (d) (yellow dots indicate individual surveyed points). Color bar with transparency and contour lines applies to all panels. Depths are relative to the NAVD88.

northerly short wind waves and swell waves approaching from the south.

Figure 3a shows the initially presumed bathymetry. As can be seen, it contains very little information about the true morphological state, it only respects depths for $x > 400m$ (not shown), and around the shoreline, $x \approx 100m$. The final estimate, after six assimilation cycles, is shown in Figure 3b. In situ surveys from the Sept. 6th and 15th, in (c) and (d) allow a qualitative evaluation of the result.

First, it stands out the ability of the system to retrieve the subaquatic orientation of the beach, in the form of an oblique nearshore terrace (between 1 and $3m$ depth contours) that was initially inexistent. Besides, it estimates correctly the position and amplitude of the sandbar and its interruption by a channel, between $y \approx 800m$ and $y \approx 950m$, where Haller et al. (2014) observed a morphologically controlled rip current during low tide.

Outside the surf zone, the result is less accurate and is followed by an increase in uncertainty (indicated by the color bar transparency). Results are not as satisfactory for $y < 650m$, where the FRF pier pilings induce scour. A visual inspection of optical data showed wave breaking was less frequent in that region. Thus, the mismatch is presumably due to unmodeled local phenomena, rather than measurement errors.

A further comparison is shown in Figure 4a. Regardless of which of the surveyed bathymetries should represent the true state for Sep. 10th, it can be seen that surf zone

inverted depths show little bias (mean bias less than $10cm$ deep in both cases). Finally, Figure 4b shows the root mean squared error evolution over time. This reflects that much of the correction is done during the first assimilation cycles, showing that for operational purposes, this approach should be able to work under rapidly changing bathymetry and that it could recover fast after periods of blackout or missed data.

DISCUSSION
Although promising, an important assumption remains in the present methodology, namely the model errors. Here, they have been assumed to stem only from uncertain
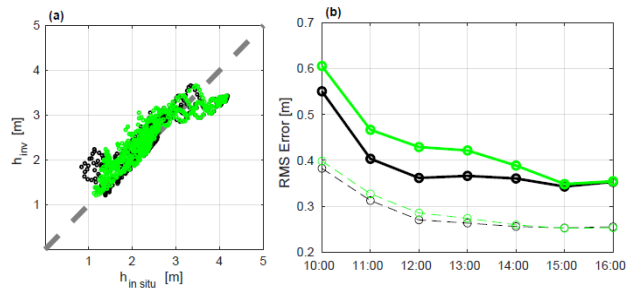

Figure 4. Comparison of surveyed surf zone depths ($140 < x < 260m, y > 650m$) from 6 Sep. (green) and 15 Sep. (black) to inverted depths (a). Dashed gray line denotes perfect agreement. Root mean squared deviation evolution for the whole domain (dashed lines) and surf zone (solid lines), following the same color scheme.

bathymetry, whereas boundary conditions and model physics have been assumed perfect. For instance, SWAN has been used as a stand-alone model and the effects of currents on waves have been completely neglected. But most notably, the offshore wave spectral boundary conditions have been specified from in situ measurements. At other sites, these would be acquired from larger-scale forecasts, which would likely have more error. Thus, an interesting extension of this work would be the inclusion of bathymetric and wave boundary conditions errors. Wilson and Berezhnoy (2018) have already tackled this problem on an alongshore uniform setup.

CONCLUSIONS

The present work shows a new application of the ensemble Kalman filter to the problem of surf zone bathymetry inversion. Remotely sensed roller dissipations fields, following the approach of Díaz et al. (2018), were assimilated to update model predictions. After a six hour application, the system was able to retrieve improved bathymetric estimates, without any in situ depth measurement. This contrast with previous applications of the filter, where more than one data stream were used as observation (e.g. Wilson et al., 2014). A prominent feature of this approach is its ability to reliably capture the amplitude and position of nearshore sandbars. This suggests applications where the nearshore bathymetry could be continuously monitored only from remote sensing data.

REFERENCES

Aarninkhof, Ruessink, Roelvink (2005). Nearshore subtidal bathymetry from time-exposure video images. Journal of Geophysical Research, 110, 2005

Battjes, Janssen (1978). Energy loss and set-up due to breaking random waves. Proceedings of the 16th International Conference on Coastal Engineering

Booij, Ris, Holthuijsen (1999). A third-generation wave model for coastal regions, Part I, Model description and validation. J. Geophys. Res.. 104.7649-7656.

Brodie, Palmsten, Hesser, Dickhudt, Raubenheimer, Ladner, Elgar (2018). Evaluation of video-based linear depth inversion performance and applications using altimeters and hydrographic surveys in a wide range of environmental conditions. Coastal Engineering. 136.

Catalán, Haller, Holman, Plant (2011). Optical and Microwave Detection of Wave Breaking in the Surf Zone. Geoscience and Remote Sensing, IEEE Transactions on. 49. 1879 - 1893.

Catalán, Haller (2008). Remote sensing of breaking wave phase speeds with app lication to nonlinear depth inversion. Coastal Engineering. 55. 93-111.

Dally, Brown (1995). A modeling investigation of the breaking wave roller with application to cross-shore currents. Journal of Geophysical Research. 1002. 24873-24884.

Díaz, Catalán, Wilson (2018). Quantification of Two-Dimensional Wave Breaking Dissipation in the Surf Zone from Remote Sensing Data. Remote Sensing. 10. 38. 10.3390/rs10010038.

Duncan (1981). An experimental investigation of breaking waves produced by a towed hydrofoil. Proc. R. Soc. Lond. A, 377, 331-348.

Haller, Honegger, Catalán (2014). Rip Current Observations via Marine Radar. Journal of Waterway Port Coastal and Ocean Engineering. 140. 115-124.

Holman, Haller (2013). Remote Sensing of the Nearshore. Annual review of marine science. 5.

Holman, Plant, Holland (2013). CBathy: A robust algorithm for estimating nearshore bathymetry. Journal of Geophysical Research: Oceans. 118.

Holman, Stanley (2007). The history and technical capabilities of Argus. Coastal Engineering. 54. 477-491.

Long (1996). Index and bulk parameters for frequency-directional spectra measured at CERC Field Research Facility, July 1994 to August 1995, Misc. Pap. CERC-96-6, U.S. Army Eng. Waterw. Exp. Stn., Vicksburg, Miss.

Reniers, Roelvink, Thornton (2004). Morphodynamic modeling of an embayed beach under wave group forcing. Journal of Geophysical Research.

van Dongeren , Plant , Cohen , Roelvink , Haller , Catalán (2008). Beach Wizard: Nearshore bathymetry estimation through assimilation of model computations and remote observations. Coastal Engineering. 55. 1016-1027.

Wilson, Özkan-Haller, Holman, Haller, Honegger, Chickadel (2014). Surf Zone Bathymetry and Circulation Predictions via Data Assimilation of Remote Sensing Observations. Journal of Geophysical Research: Oceans. 119.

Wilson, Berezhnoy (2018). Surfzone State Estimation, with Applications to Quadcopter-Based Remote Sensing Data. Journal of Atmospheric and Oceanic Technology. 35.